Conventional and unconventional photon blockade effects in quantum optomechanics

Xiang-Xiang Lu, Jia Ni, Feng-Chao Wang[†], Yi-Gui Li[‡], Ling-Juan Feng[§]

School of Sciences, Shanghai Institute of Technology, Shanghai 201418, China
Corresponding authors. E-mail: [†]fcwang@sit.edu.cn, [‡]ygli@sit.edu.cn, [§]lingjuanfeng@sit.edu.cn
Received January 21, 2025; accepted June 13, 2025

ABSTRACT

We theoretically study the photon blockade (PB) effect in a double-cavity optomechanical system with the two-photon driving. By analytical calculations and numerical simulations, the physical mechanisms of conventional photon blockade (CPB) and unconventional photon blockade (UPB) are discussed in detail. And then we obtain the optimal parameter conditions for PB. In our work, there exist both the CPB induced by strong nonlinear interaction and the UPB caused by quantum interference. In particular, we find that CPB and UPB can occur simultaneously under the same parameters. In addition, we also prove that the appropriate values of nonreciprocal coupling and two-photon driving are favorable to the improvement of PB. Our proposal provides an idea for simultaneously realizing CPB and UPB in the optomechanical system and offers a route for constructing high-quality single-photon sources.

Keywords conventional photon blockade, unconventional photon blockade, two-photon driving

1 Introduction

Photon blockade (PB), an antibunching effect resulting from the excitation of the first photon blocking the injection of the second photon, is a prominent technique for generating single-photon sources. In general, there are two main schemes to realize photon antibunching, i.e., conventional photon blockade (CPB) [1–17] and unconventional photon blockade (UPB) [18–33], which are based on the anharmonic eigenenergy of the system and the destructive quantum interference in two-photon excitation processes, respectively. For CPB, strong nonlinearity (or strong coupling to nonlinear elements like atoms) is generally a prerequisite for realizing PB, which has been experimentally achieved in cavity quantum electrodynamics (QED) [1–6] and circuit QED systems [7, 8].

Compared with CPB, UPB can relax the requirement for strong nonlinearity, which offers a helpful way to achieve photon antibunching and reveal quantum correlation properties in weak-parameter devices. Usually, UPB originates from destructive quantum interference between distinct excitation pathways [18, 19]. Based on this mechanism, UPB has been studied theoretically and experimentally in different systems, such as superconducting resonators [20], second-order nonlinearity [21, 22], parametric interactions [23], non-Markovian reservoir [24], cavity QED system [25–27], optomechanical system [28–31], and magnons [32, 33].

Recently, some works have discovered that both CPB and UPB can occur in the same quantum system, and have analyzed the physical mechanisms behind CPB and UPB [34–40]. For example, they can be understood as the interference between squeezed and coherent components [40]. Generally, the single-photon source based on CPB has the advantage of high mean photon number (brightness), but relatively poor purity. By contrast, the one based on UPB has high purity but poor brightness.

Further, under the same parameter conditions, two types of PB have been realized simultaneously in the cavity QED system [41–44] and coupled cavities with Kerr nonlinearity [45, 46].

Motivated by the above-mentioned works [34–46], we are going to explore CPB and UPB in the optomechanical system. Specifically, we consider the optomechanical system consisting of two mechanical modes and two optical modes in the presence of both one and two-photon driving. Then, we analyze the influences of the coupling between two cavities, two-photon driving, and optomechanical coupling on PB. The results demonstrate that both CPB and UPB are simultaneously achieved in the stronger coupling regime. To further relax the coupling strength, we choose the nonreciprocal coupling between two cavities. In this case, we also find that CPB and UPB can be simultaneously realized in the strong coupling regime. Thus, this approach can relax the couplings required for CPB and UPB from the stronger to strong coupling. Our proposal combines the advantages of CPB and UPB and provides a promising method to generate the single-photon source with high purity and brightness in optomechanics.

The remainder of this paper is organized as follows. In Section 2, we present the theoretical model and system Hamiltonian. Then, the validity of Hamiltonian and the effect of thermal noise on PB are discussed by the master equation and second-order correlation function. In Section 3, we calculate analytically the Schrödinger equation and derive the mean photon number and second-order correlation function. Subsequently, the physical mechanisms of CPB and UPB have been explained in detail. Most importantly, we combine CPB with UPB successfully. In Section 4, we also investigate the effects of nonreciprocal coupling and two-photon driving on PB, respectively. Finally, we provide the experimental feasibility and summarize the whole work in Section 5.

2 Theoretical model

As shown in Fig. 1, we consider a double-cavity optomechanical system, which contains two mechanical oscillators and two optical cavities. Besides the optomechanical interaction coupling the mechanical oscillator to the optical cavity, these two optical cavities with the two-photon (i.e., parametric) driving [23–25, 47] are coupled by the nonreciprocal interaction [35, 36, 48–50]. In a frame rotating with the driving frequency ω_l, the Hamiltonian of this system can be written as (setting $\hbar = 1$)

$$H_1 = \sum_{j=1}^{2} [-\Delta_j a_j^\dagger a_j + \omega_{m_j} b_j^\dagger b_j - g_j a_j^\dagger a_j (b_j^\dagger + b_j) + i\lambda_j a_j^{\dagger 2}$$
$$- i\lambda_j a_j^2] + E(a_1^\dagger + a_1) + \mu_1 a_1^\dagger a_2 + \mu_2 a_2^\dagger a_1, \quad (1)$$
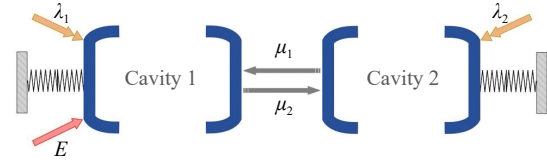
Fig. 1 Schematic diagram of the double-cavity optomechanical system with single- and two-photon driving, as well as nonreciprocal coupling.

where $a_j(a_j^\dagger)$ is the annihilation (creation) operator of the jth optical cavity with the frequency ω_j, and $b_j(b_j^\dagger)$ is the annihilation (creation) operator of the jth mechanical oscillator with the frequency ω_{m_j}. $\Delta_j = \omega_l - \omega_j$ is the detuning of the jth cavity from the laser drive. g_j is the coupling strength between the cavity a_j and the mechanical oscillator b_j. λ_j is the two-photon driving term. The amplitude of the driven laser field is described by $|E| = \sqrt{2\kappa_1 P/(\hbar\omega_l)}$ with the power P and corresponding cavity decay rate κ_1. μ_j denotes the tunneling strength of photon hopping between cavities a_j. Here, this hopping is nonreciprocal (i.e., asymmetric, $\mu_1 \neq \mu_2$), which can be achieved via non-Hermiticity [51–53], nanoparticles [54], quantum impurity [55], optical delay lines [56], reservoir engineering [57], and so on. For example, the nonreciprocal coupling is scaled by $\exp(\pm h)$ in opposite directions with h being the effect of imaginary vector potential [51–53].

In a displaced oscillator representation defined by the unitary operator $U = \exp\left[\sum_{j=1}^{2} \frac{g_j}{\omega_{m_j}} a_j^\dagger a_j \left(b_j^\dagger - b_j\right)\right]$ [35, 36, 58–60], the transformed Hamiltonian can be derived as

$$H_2 = \sum_{j=1}^{2} [-\Delta_j a_j^\dagger a_j + \omega_{m_j} b_j^\dagger b_j - \eta_j a_j^\dagger a_j a_j^\dagger a_j + i\lambda_j a_j^{\dagger 2}$$
$$- i\lambda_j a_j^2] + E(a_1^\dagger + a_1) + \mu_1 a_1^\dagger a_2 + \mu_2 a_2^\dagger a_1, \quad (2)$$

with $\eta_j = g_j^2/\omega_{m_j}$ ($j = 1, 2$, and $g_j \ll \omega_{m_j}$) being the Kerr-type nonlinear coupling. Here, the mechanical oscillators have been decoupled from the optical cavities. This indicates that the evolution of optical and mechanical parts is independent of each other. Thus, the mechanical part in Eq. (2) can be ignored safely when we study the optical properties of the system. The effective Hamiltonian can be given by

$$H_3 = \sum_{j=1}^{2} [-\Delta_j a_j^\dagger a_j - \eta_j (a_j^\dagger a_j)^2 + i\lambda_j a_j^{\dagger 2} - i\lambda_j a_j^2]$$
$$+ E(a_1^\dagger + a_1) + \mu_1 a_1^\dagger a_2 + \mu_2 a_2^\dagger a_1, \quad (3)$$

where this Hamiltonian describes a pure optical system consisting of two optical modes a_1 and a_2.

Here, we numerically study the quantum dynamics of the optomechanical or optical system and then employ

012202-2

Xiang-Xiang Lu, et al., Front. Phys. 21(1), 012202 (2026)

the master equations for the system density operator ρ defined by

$$\dot{\rho} = -\mathrm{i}[H_1, \rho] + \frac{\kappa_1}{2}L[a_1]\rho + \frac{\kappa_2}{2}L[a_2]\rho + \frac{\gamma_1}{2}(n_{th}+1)L[b_1]\rho$$
$$+ \frac{\gamma_2}{2}(n_{th}+1)L[b_2]\rho + \frac{\gamma_1}{2}n_{th}L[b_1^\dagger]\rho + \frac{\gamma_2}{2}n_{th}L[b_2^\dagger]\rho,$$
$$\dot{\rho} = -\mathrm{i}[H_3, \rho] + \frac{\kappa_1}{2}L[a_1]\rho + \frac{\kappa_2}{2}L[a_2]\rho,$$

$$(4)$$

where $L[o]\rho = 2o\rho o^\dagger - o^\dagger o\rho - \rho o^\dagger o$ $(o = a_1, a_2, b_1, b_2)$ is the Liouvillian operator for the two optical cavities and two mechanical modes. $n_{th} = 1/\left[\exp\left(\hbar\omega_{m_j}/(k_B T)\right) - 1\right]$ denotes the thermal phonon number of mechanical mode at the environmental temperature T with the Boltzmann constant k_B. κ_j and γ_j represent the decay rate of cavity and the damping rate of mechanical oscillator $(j = 1, 2)$, respectively. When the present system is in the steady or transient state, the corresponding second-order correlation function in the a_1 mode can be evaluated by $g_{ss}^{(2)}(0) = \lim_{t\to\infty}\langle a_1^\dagger a_1^\dagger a_1 a_1\rangle(t)/\langle a_1^\dagger a_1\rangle^2(t)$ or $g^{(2)}(0) = \langle a_1^\dagger a_1^\dagger a_1 a_1\rangle(t)/\langle a_1^\dagger a_1\rangle^2(t)$ [61]. Here, the condition $g_{ss}^{(2)}(0) < 1$ $[g^{(2)}(0) < 1]$ characterizes photon antibunching. Particularly, when $g_{ss}^{(2)}(0) \to 0$ $[g^{(2)}(0) \to 0]$, the perfect photon blockade (PB) will occur in the optical mode a_1.

In order to check the validity of this effective Hamiltonian in Eq. (3), we plot in Fig. 2 the time evolution of $g^{(2)}(0)$, which is calculated by the master equations, given in Eq. (4). In the numerical simulation, we can regulate the system parameters to satisfy the conditions for $\gamma < \kappa$ and $g_j \ll \omega_{m_j}$, and compute on the truncated Hilbert space of dimensions $(N_{a_1} \times N_{a_2} \times N_{b_1} \times N_{b_2})^2$ or $(N_{a_1} \times N_{a_2})^2$ in the optomechanical or optical system, where $N_{a_1} = N_{a_2} = N_{b_1} = N_{b_2} = 4$. From Fig. 2, it is clear to see that the approximate results obtained from effective Hamiltonian H_3 (dashed curve) are in good agreement with the exact numerical results of full Hamiltonian H_1 (solid curve). We also find that when $\kappa t \approx 20$, the correlation function $g^{(2)}(0)$ approaches a steady value. For the dissipation rate $\kappa = 0.1$ MHz, the relaxation time of the system is about 200 μs.

In the discussions above, we focus on the case of zero temperature $(n_{th} = 0)$. However, in the strong or stronger coupling regime, the mechanical thermal noise may affect the PB and cannot be neglected. Therefore, in Fig. 3, we investigate the influence of thermal phonon number n_{th} on the second-order correlation function $g_{ss}^{(2)}(0)$ based on Eq. (4) with H_1. For the system parameters Δ and μ, we choose the optimal parameters Δ_{opt} and μ_{opt}, as shown in Section 3. Specifically, in the strong coupling regime $(\eta = 10\kappa)$, the value of $g_{ss}^{(2)}(0)$ sharply increases with the increase of thermal phonon number n_{th}. Eventually, the PB (or photon antibunching) can disappear for very small thermal phonon numbers, i.e., $g_{ss}^{(2)}(0) > 1$. This suggests that the mechanical thermal
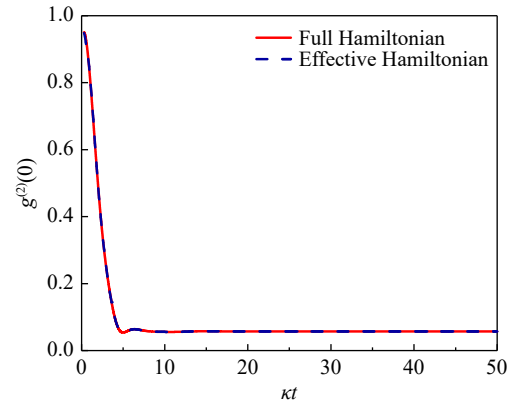

Fig. 2 The second-order correlation function $g^{(2)}(0)$ versus the time κt with the parameters $\kappa_1 = \kappa_2 = \kappa$, $\gamma_1 = \gamma_2 = \gamma = 0.01\kappa$, $\Delta_1 = \Delta_2 = \Delta = -0.76\kappa$, $\eta_1 = \eta_2 = \eta = 0.88\kappa$, $\omega_{m_1} = \omega_{m_2} = 10^7\gamma$, $\mu_1 = \mu_2 = \mu = 0.7\kappa$, $\lambda_1 = \lambda_2 = \lambda = 1 \times 10^{-6}\kappa$, $n_{th} = 0$, and $E = 0.02\kappa$.
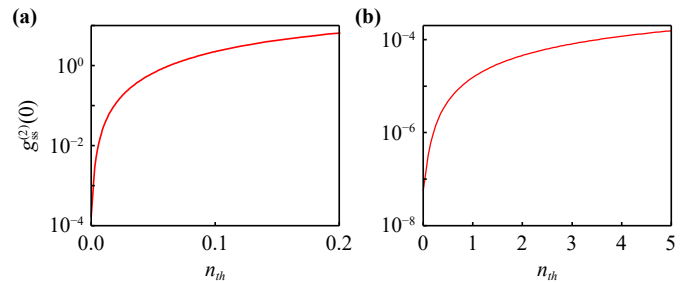

Fig. 3 The second-order correlation function $g_{ss}^{(2)}(0)$ versus the thermal phonon number n_{th} for different values of η, Δ and μ considered as: **(a)** $\eta = 10\kappa$, $\Delta_{\mathrm{opt}} = -28\kappa$, $\mu_{\mathrm{opt}} = 23\kappa$, and **(b)** $\eta = 10^2\kappa$, $\Delta_{\mathrm{opt}} = -251\kappa$, $\mu_{\mathrm{opt}} = 151\kappa$. Other system parameters are the same as that in Fig. 2 except for $n_{th} \neq 0$ and $E = 0.01\kappa$.

noise has an undesirable effect on the PB. But in the stronger coupling regime $(\eta = 10^2\kappa)$, the PB can survive in the finite thermal phonon number.

3 Analytical calculation and photon blockade with $\mu_1 = \mu_2$ and $\lambda \neq 0$

To investigate the PB phenomenon in detail, we use the mean photon number and second-order correlation function, which can be obtained by analytically calculating the Schrödinger equation $\mathrm{i}\frac{\mathrm{d}|\psi\rangle}{\mathrm{d}t} = H_{\mathrm{eff}}|\psi\rangle$. When the optical decay κ_j is phenomenologically introduced to H_3, the effective non-Hermitian Hamiltonian [36, 62–64] takes the form

$$H_{\mathrm{eff}} = H_3 - \frac{\mathrm{i}\kappa_1}{2}a_1^\dagger a_1 - \frac{\mathrm{i}\kappa_2}{2}a_2^\dagger a_2. \qquad (5)$$

In the weak-driving regime $(E \ll \kappa_j)$, only few photons (such as a single photon or two photons) in the

Xiang-Xiang Lu, et al., Front. Phys. 21(1), 012202 (2026)

012202-3

cavity will be excited. Thus, the wave function of the system can be approximately expanded to the following form:

$$|\psi\rangle = C_{00}|00\rangle + C_{01}|01\rangle + C_{10}|10\rangle + C_{11}|11\rangle$$
$$+ C_{02}|02\rangle + C_{20}|20\rangle, \tag{6}$$

with the probability amplitudes $C_{N_{a_1} N_{a_2}}$ of the state $|N_{a_1} N_{a_2}\rangle$. Here, $|N_{a_1}\rangle$ and $|N_{a_2}\rangle$ are the number states for the a_1 and a_2 modes, respectively.

Substituting the state $|\psi\rangle$ and the Hamiltonian H_{eff} into the Schrödinger equation, we can obtain a set of evolution equations:

$$i\dot{C}_{00} = EC_{10} - i\sqrt{2}\lambda_2 C_{02} - i\sqrt{2}\lambda_1 C_{20},$$

$$i\dot{C}_{01} = \mu_2 C_{10} + EC_{11} - \Delta_2 C_{01} - \eta_2 C_{01} - \frac{i\kappa_2}{2}C_{01},$$

$$i\dot{C}_{10} = \mu_1 C_{01} + EC_{00} + \sqrt{2}EC_{20} - \Delta_1 C_{10} - \eta_1 C_{10}$$
$$- \frac{i\kappa_1}{2}C_{10},$$

$$i\dot{C}_{11} = \sqrt{2}\mu_1 C_{02} + \sqrt{2}\mu_2 C_{20} + EC_{01} - \Delta_1 C_{11} - \Delta_2 C_{11}$$
$$- \eta_1 C_{11} - \eta_2 C_{11} - \frac{i\kappa_1}{2}C_{11} - \frac{i\kappa_2}{2}C_{11},$$

$$i\dot{C}_{02} = \sqrt{2}\mu_2 C_{11} + i\sqrt{2}\lambda_2 C_{00} - 2\Delta_2 C_{02} - 4\eta_2 C_{02}$$
$$- i\kappa_2 C_{02},$$

$$i\dot{C}_{20} = \sqrt{2}\mu_1 C_{11} + \sqrt{2}EC_{10} + i\sqrt{2}\lambda_1 C_{00} - 2\Delta_1 C_{20}$$
$$- 4\eta_1 C_{20} - i\kappa_1 C_{20}. \tag{7}$$

For mathematical simplicity, we set $\Delta_1 = \Delta_2 = \Delta$, $\lambda_1 = \lambda_2 = \lambda$, $\eta_1 = \eta_2 = \eta$, $\mu_1 = \mu_2 = \mu$ and $\kappa_1 = \kappa_2 = \kappa$. Under the weak-driving condition, these probability amplitudes meet the relations of $|C_{N_{a_1} N_{a_2}}|(N_{a_1} + N_{a_2} = 2) \ll |C_{N_{a_1} N_{a_2}}|(N_{a_1} + N_{a_2} = 1) \ll |C_{00}| \simeq 1$. By neglecting the higher-order terms, the steady-state solutions (i.e., $t \to \infty$) for the amplitudes $C_{N_{a_1} N_{a_2}}$ are given as

$$C_{01} = \frac{-E\mu}{-M^2 + \mu^2}, \tag{8}$$

$$C_{10} = \frac{-EM}{-M^2 + \mu^2}, \tag{9}$$

$$C_{11} = \frac{-\mu(2i\lambda\mu^2 - E^2 M - 2i\lambda M^2 - E^2 N)}{B}, \tag{10}$$

$$C_{02} = \frac{E^2\mu^2(M+N) - 2i\lambda\mu^2 MN + 2i\lambda M^3 N}{\sqrt{2}NB}, \tag{11}$$

$$C_{20} = -(E^2\mu^2 M - E^2\mu^2 N + 2i\mu^2 MN - 2E^2 M^2 N$$
$$- 2i\lambda M^3 N)/(\sqrt{2}NB), \tag{12}$$

with $M = \Delta + \frac{i\kappa}{2} + \eta$, $N = \Delta + \frac{i\kappa}{2} + 2\eta$ and $B = 2(M^2 - \mu^2)(-\mu^2 + MN)$. Here, the full analytical results for optimal conditions (λ_{opt} and μ_{opt}) of $C_{20} = 0$ are too long to be given. However, it is possible to obtain the simple relation for $\Delta = 0$ as

$$\lambda_{\text{opt}} = \frac{E^2(160\eta^4 + 4\eta^2\kappa^2 + 3\kappa^4 + \sqrt{G})}{4\kappa(64\eta^4 + 20\eta^2\kappa^2 + \kappa^4)}, \tag{13}$$

where $G = 25600\eta^8 + 21760\eta^6\kappa^2 + 6352\eta^4\kappa^4 + 24\eta^2\kappa^6 - 7\kappa^8$. For weak or strong coupling ($\eta < \kappa$ or $\eta > \kappa$), we have the approximate expression: $\lambda_{\text{opt}} \sim E^2/\kappa$. For $\Delta \neq 0$, we also have the similar results.

Then, the mean photon number of optical cavity a_1 can be analytically obtained via Eqs. (8)–(12) as

$$\langle n \rangle = \langle a_1^\dagger a_1 \rangle$$
$$= |C_{10}|^2 + |C_{11}|^2 + 2|C_{20}|^2$$
$$\approx |C_{10}|^2. \tag{14}$$

And the second-order correlation function in the steady state is given by

$$g_{ss}^{(2)}(0) = \frac{\langle a_1^{\dagger 2} a_1^2 \rangle}{\langle a_1^\dagger a_1 \rangle^2}$$
$$= \frac{2|C_{20}|^2}{(|C_{10}|^2 + |C_{11}|^2 + 2|C_{20}|^2)^2}$$
$$\approx \frac{2|C_{20}|^2}{|C_{10}|^4}. \tag{15}$$

We first discuss quantum interference-induced photon blockade (or more accurately unconventional photon blockade, UPB) in our system with $\mu_1 = \mu_2$ and $\lambda \neq 0$. According to the expression for the second-order correlation function (15), if $C_{20} = 0$, we have $g_{ss}^{(2)}(0) = 0$. In other word, the realization of UPB requires that the real and imaginary parts of C_{20} should be equal to zero at the same time. After some straightforward calculations, we obtain two sets of the optimal UPB conditions for Δ_{opt} and μ_{opt}. However, these analytical results are too long to be presented here. Specifically, when the system parameters are considered as $E = 0.01\kappa$ and $\lambda = 1 \times 10^{-6}\kappa$, we get one set of optimal parameters: for the weak coupling ($\eta = 0.1\kappa$), $\Delta_{\text{opt}} \approx 0.15\kappa$ and $\mu_{\text{opt}} \approx 1.9\kappa$; for the strong coupling ($\eta = 10\kappa$), $\Delta_{\text{opt}} \approx -10\kappa$ and $\mu_{\text{opt}} \approx 0.7\kappa$; for the stronger coupling ($\eta = 10^2\kappa$), $\Delta_{\text{opt}} \approx -10^2\kappa$ and $\mu_{\text{opt}} \approx 0.7\kappa$. Similarly, the other set of optimal parameters is obtained as follows: for $\eta = 0.1\kappa$, $\Delta_{\text{opt}} \approx -2\kappa$ and $\mu_{\text{opt}} \approx 12.8\kappa$; for $\eta = 10\kappa$, $\Delta_{\text{opt}} \approx -28\kappa$ and $\mu_{\text{opt}} \approx 23\kappa$; for $\eta = 10^2\kappa$, $\Delta_{\text{opt}} \approx -251\kappa$ and $\mu_{\text{opt}} \approx 151\kappa$.

In Fig. 4, we plot the second-order correlation function $g_{ss}^{(2)}(0)$ as a function of the detuning Δ/κ in weak coupling regime ($\eta = 0.1\kappa$). Figure 4 shows that except for the minimal value of $g_{ss}^{(2)}(0)$, the analytical results (solid curves) in Eq. (15) agree well with the numerical
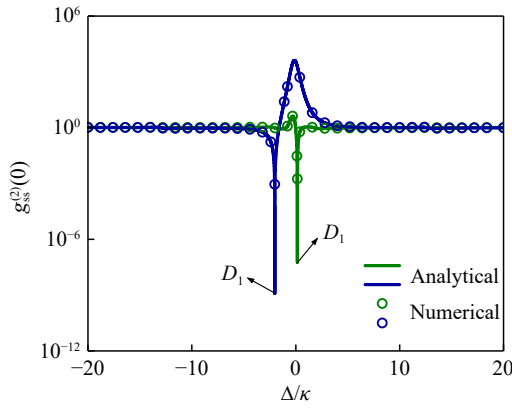
012202-4

Xiang-Xiang Lu, et al., Front. Phys. 21(1), 012202 (2026)

Fig. 4 The second-order correlation function $g_{ss}^{(2)}(0)$ versus the detuning Δ/κ with the parameters $\eta = 0.1\kappa$, $E = 0.01\kappa$ and $\lambda = 1 \times 10^{-6}\kappa$. D_1 is the dip in the $g_{ss}^{(2)}(0)$ curve. The value of μ is considered to be the optimal μ_{opt}. Here, the green solid curve (or circles) denotes the first case for $\mu_{opt} \approx 1.9\kappa$, while the blue solid curve (or circles) corresponds to the second case for $\mu_{opt} \approx 12.8\kappa$.
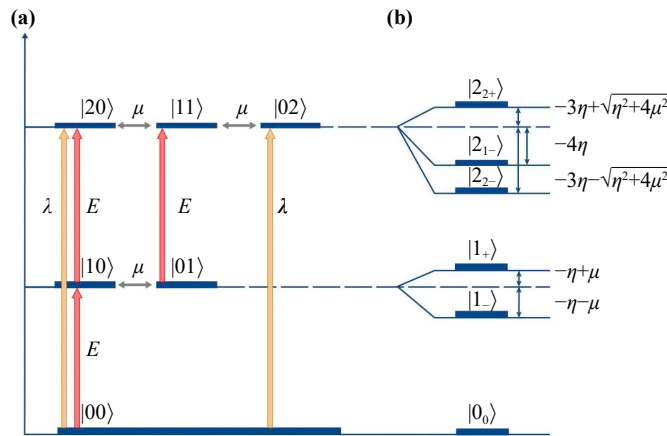

Fig. 5 Energy-level diagrams of **(a)** bare states and **(b)** eigenstates.

results (circles) using the master Eq. (4) and H_3. This difference between two minimal values is mainly attributed to the Hilbert-space truncation. In the analytical derivation, we retain only the state $|N_{a_1} N_{a_2}\rangle$ with $N_{a_1} + N_{a_2} \leq 2$. But in the numerical simulation, the Hilbert space is truncated into finite dimensions $(N_{a_1} \times N_{a_2})^2$, where $N_{a_1} = N_{a_2} = 10$. Moreover, it clearly shows that the global minimum of $g_{ss}^{(2)}(0)$ is located at the optimal value of $\Delta_{opt} \approx 0.15\kappa$, -2κ. This feature (the dip D_1, $g_{ss}^{(2)}(0) \ll 1$) shows strong photon antibunching, which indicates the occurrence of UPB. In this situation, the physical mechanism behind UPB can be understood from quantum interference effect and is illustrated in more detail in Fig. 5(a). The interference can happen between the four different transition pathways for two-photon excitation: two direct transitions $|10\rangle \xrightarrow{E} |20\rangle$ and
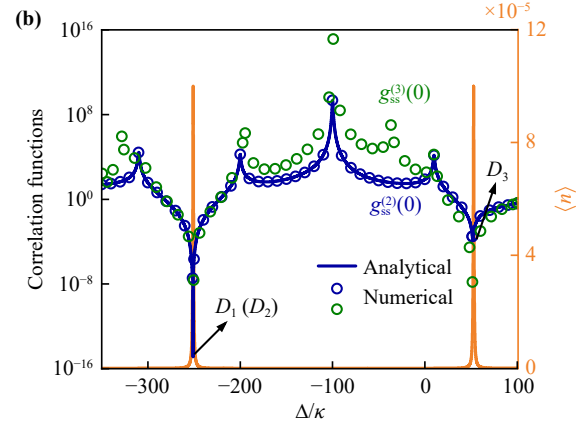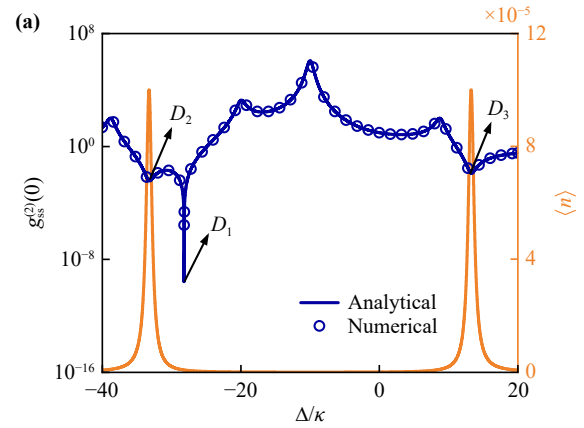
Fig. 6 The second- and third-order correlation functions $g_{ss}^{(2)}(0)$, $g_{ss}^{(3)}(0)$ and the mean photon number $\langle n \rangle$ versus the detuning Δ/κ with the parameters $E = 0.01\kappa$ and $\lambda = 1 \times 10^{-6}\kappa$. **(a)** $\eta = 10\kappa$, **(b)** $\eta = 10^2\kappa$. D_1, D_2, and D_3 are the dips in the $g_{ss}^{(2)}(0)$ and $g_{ss}^{(3)}(0)$ curves.

$|00\rangle \xrightarrow{\lambda} |20\rangle$, and two coupling-mediated transitions $|10\rangle \xleftrightarrow{\mu} |01\rangle \xrightarrow{E} (|11\rangle \xleftrightarrow{\mu} |02\rangle) \xleftrightarrow{\mu} |20\rangle$ and $|00\rangle \xrightarrow{\lambda} |02\rangle \xleftrightarrow{\mu} |11\rangle \xleftrightarrow{\mu} |20\rangle$. If the system parameters meet the optimal condition (i.e., $C_{20} = 0$), these transition pathways will destructively interfere, resulting in the complete suppression of two-photon excitation. We also find in Fig. 4 that the second case can be able to produce stronger antibunching than the first case. Similarly, for $\eta = 10\kappa$, $10^2\kappa$, there are results like the case ($\eta = 0.1\kappa$). For this, we mainly focus on studying the effect of the second case on PB in the following discussion.

Next, we consider the strong coupling regime, e.g., $\eta = 10\kappa$. In Fig. 6(a), we depict the second-order correlation function $g_{ss}^{(2)}(0)$ and the mean photon number $\langle n \rangle$ as functions of the detuning Δ/κ. For strong coupling, we clearly observe that there are three dips [D_1, D_2, and D_3 in Fig. 6(a)] located at $\Delta_{opt} \approx -28\kappa$, -33κ, and 13κ, respectively. For the dip D_1, there is a minimized value of $g_{ss}^{(2)}(0)$. Here, the system parameters Δ and μ can satisfy the optimal condition $C_{20} = 0$. Apparently, this feature belongs to the UPB. In addition, there also exist two same minima of $g_{ss}^{(2)}(0)$ at two dips D_2 and D_3,

Xiang-Xiang Lu, et al., Front. Phys. 21(1), 012202 (2026)

012202-5

corresponding to two peaks of the mean photon number $\langle n \rangle$ (shown by the orange solid curve). These behaviors are different from the UPB, which can be explained as follows. We begin by analyzing the low-energy level structure of the eigenstates of the present system [see Fig. 5(b)]. Without considering the single- and two-photon drivings, we diagonalize the Hamiltonian $H_{\mathrm{ND}} = \omega_1 a_1^\dagger a_1 + \omega_2 a_2^\dagger a_2 - \eta_1 (a_1^\dagger a_1)^2 - \eta_2 (a_2^\dagger a_2)^2 + \mu_1 a_1^\dagger a_2 + \mu_2 a_2^\dagger a_1$, in the few-photon subspace, yielding the energy eigenstates and eigenvalues. Here, we still assume $\omega_1 = \omega_2 = \omega$, $\eta_1 = \eta_2 = \eta$, and $\mu_1 = \mu_2 = \mu$. In the zero-photon subspace, the corresponding eigenstate and eigenvalue are $|0_0\rangle = |00\rangle$ and 0. In the one-photon subspace, there are $|1_\pm\rangle = 1/\sqrt{2}(|01\rangle \pm |10\rangle)$ and $\omega - \eta \pm \mu$. In the two-photon subspace, $|2_{1-}\rangle = 1/\sqrt{2}(|02\rangle - |20\rangle)$ and $2\omega - 4\eta$, $|2_{2\pm}\rangle = N_\pm [|02\rangle + |20\rangle + \frac{\eta \pm \sqrt{\eta^2 + 4\mu^2}}{\sqrt{2}\mu}|11\rangle]$ and $2\omega - 3\eta \pm \sqrt{\eta^2 + 4\mu^2}$, where $N_\pm = 1/\sqrt{2 + (\frac{\eta \pm \sqrt{\eta^2 + 4\mu^2}}{\sqrt{2}\mu})^2}$ is the normalization constant. In this case, the driving frequency is resonantly (i.e., $\Delta = -\eta - \mu$) coupled to the $|0_0\rangle \to |1_-\rangle$ transition, but the subsequent transition $|1_-\rangle \to |2_{1-}\rangle$ or $|2_{2+}\rangle$ is suppressed due to large detuning $2(\mu - \eta)$ or $\sqrt{\eta^2 + 4\mu^2} + 2\mu - \eta$. Likewise, when $\Delta = -\eta + \mu$, two-photon excitation process can also be suppressed. Thus, the large detuning can lead to the anharmonicity of the energy-level structure, which explains the essence of conventional photon blockade (CPB). More importantly, by comparing these dips D_1 and D_2 (or D_3) in the $g_{\mathrm{ss}}^{(2)}(0)$ curve, it is clear that the minimized value of $g_{\mathrm{ss}}^{(2)}(0)$ in UPB is much lower than in CPB. However, from the $\langle n \rangle$ curve, we find that the mean photon number in CPB is much higher than in UPB. That is to say, a single photon generated by UPB has high purity, but that by CPB has high brightness.

To achieve CPB and UPB simultaneously, we need to further increase the coupling strength. For example, we choose the stronger coupling with $\eta = 10^2 \kappa$. From Fig. 6(b), we find that there are only two dips D_1 (D_2) and D_3 in the $g_{\mathrm{ss}}^{(2)}(0)$ and $g_{\mathrm{ss}}^{(3)}(0)$ curves. Specifically, the right one D_3 is the location of the CPB appearing, which corresponds to the local maximum value of $\langle n \rangle$. However, the left one D_1 (D_2) can satisfy the optimal conditions for UPB and CPB, i.e., $\mu = \mu_{\mathrm{opt}}$ and $\Delta = \Delta_{\mathrm{opt}} = -\eta - \mu$. Under these conditions, the system has the strong antibunching (purity) and high mean photon number (brightness). The results indicate that the advantages of UPB and CPB can be brought together in our system. Furthermore, we also study the third-order correlation function in the steady state, i.e., $g_{\mathrm{ss}}^{(3)}(0) = \lim_{t \to \infty} \langle a_1^\dagger a_1^\dagger a_1^\dagger a_1 a_1 a_1 \rangle (t) / \langle a_1^\dagger a_1 \rangle^3 (t)$. As shown in Fig. 6(b), both $g_{\mathrm{ss}}^{(3)}(0) < 1$ and $g_{\mathrm{ss}}^{(2)}(0) < 1$ at two dips D_1 (D_2) and D_3 mean that only the one-photon emission is allowed, but the emission of two or more photons is blocked. Hence, our work can provide a promising route to produce single-photon sources with high purity and brightness.
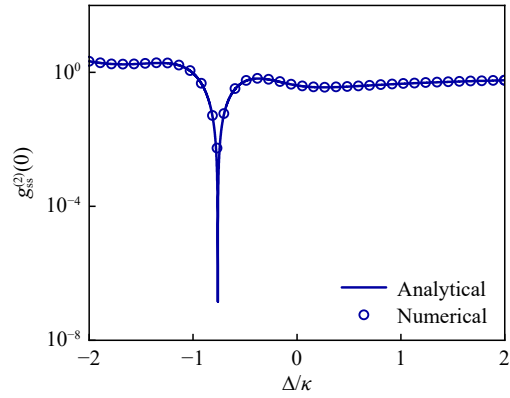

Fig. 7 The second-order correlation function $g_{\mathrm{ss}}^{(2)}(0)$ versus the detuning Δ/κ for $\eta = 0.88\kappa$ with the optimal parameter relations (Δ_{opt}, μ_{opt}). Other system parameters are set as $E = 0.02\kappa$, $\lambda = 1 \times 10^{-6}\kappa$, $\mu_2 = \kappa$ and $\mu_1 \approx 0.67\mu_2$.

4 Photon blockade with $\mu_1 \neq \mu_2$ and different λ

In the following, we will explore the performance of single-photon blockade (PB) with nonreciprocal coupling ($\mu_1 \neq \mu_2$). For the weak coupling ($\eta = 0.88\kappa$), we plot in Fig. 7 the second-order correlation function as a function of Δ/κ. We see that a strong PB is triggered at $\Delta \approx -0.76\kappa$, which satisfies the optimal conditions (Δ_{opt} and $\mu_1 = \mu_{\mathrm{opt}}$) obtained by calculating $C_{20} = 0$. This PB belongs to unconventional photon blockade (UPB). However, the corresponding results are too cumbersome to present here. For the strong coupling ($\eta = 10\kappa$), we depict in Fig. 8 the second-order correlation function $g_{\mathrm{ss}}^{(2)}(0)$ and the mean photon number $\langle n \rangle$ as functions of the detuning Δ/κ. According to the physical mechanism of conventional photon blockade (CPB), we have $\Delta_+ = -\eta + \sqrt{\mu_1}\sqrt{\mu_2}$ and $\Delta_- = -\eta - \sqrt{\mu_1}\sqrt{\mu_2}$. From Fig. 8(a), there are two dips D_1 and D_2 located at $\Delta_- = -39.8\kappa$ and $\Delta_+ = 19.8\kappa$, which correspond to the local maximum values of $\langle n \rangle$. In addition, the left one D_1 at $\Delta = \Delta_{\mathrm{opt}} = -\eta - \sqrt{\mu_1}\sqrt{\mu_2}$ also satisfies the optimal condition for UPB. This means that CPB and UPB can be obtained simultaneously in the nonreciprocal and strong coupling conditions. Similarly, D_2 at $\Delta = \Delta_{\mathrm{opt}} = -\eta + \sqrt{\mu_1}\sqrt{\mu_2}$ in Fig. 8(b) also satisfies the optimal conditions for CPB and UPB. More importantly, the stronger coupling $\eta = 10^2 \kappa$ mentioned before is not necessary to achieve CPB and UPB effects simultaneously. Therefore, our proposal is useful for relaxing the coupling condition of realizing CPB and UPB with nonreciprocal coupling.

To illustrate the influences of nonreciprocal coupling and two-photon driving on the PB effect more clearly, Figures 9 and 10 show the second-order correlation function $g_{\mathrm{ss}}^{(2)}(0)$ for different values of μ_1 and λ, respectively. From Fig. 9(a), one can observe that a strong PB effect

012202-6

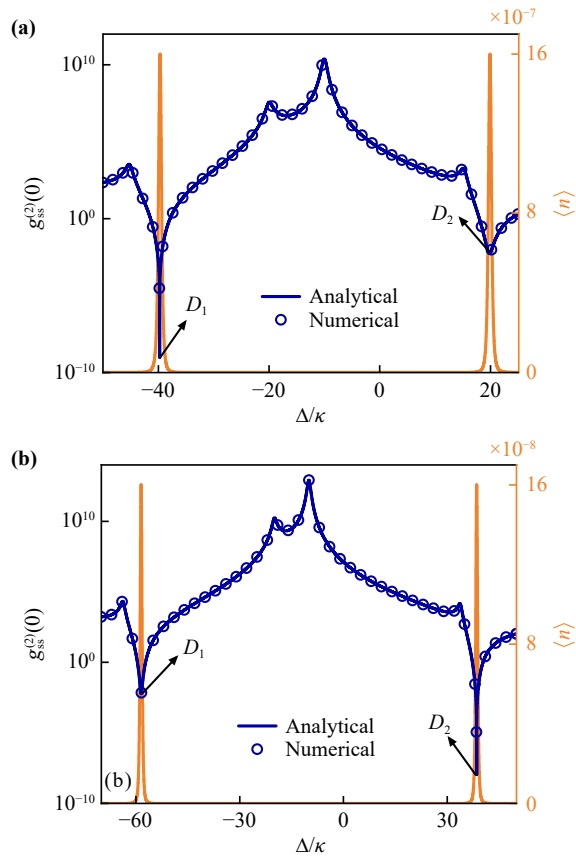Xiang-Xiang Lu, et al., Front. Phys. 21(1), 012202 (2026)

Fig. 8 The second-order correlation function $g_{ss}^{(2)}(0)$ versus the detuning Δ/κ for $\eta = 10\kappa$ with the optimal parameter relations (Δ_{opt}, μ_{opt}). Other system parameters are set as $E = 0.02\kappa$, $\lambda = 1 \times 10^{-6}\kappa$ and $\mu_2 = 1.5\kappa$. **(a)** $\mu_1 \approx 3.95 \times 10^2 \mu_2$, **(b)** $\mu_1 \approx 1.05 \times 10^3 \mu_2$.

Fig. 9 The second-order correlation function $g_{ss}^{(2)}(0)$ versus the detuning Δ/κ with different values of μ_1. The system parameters are set as $E = 0.02\kappa$ and $\lambda = 1 \times 10^{-6}\kappa$. **(a)** $\eta = 0.88\kappa$ and $\mu_2 = \kappa$, **(b)** $\eta = 10\kappa$ and $\mu_2 = 1.5\kappa$.

can be attained in the value of $\mu_1 = 0.67\mu_2$. This is because the intermediate value satisfies the optimal condition for the UPB. Under this condition, it is clear in Fig. 10(a) that the PB effect can be realized without or with two-photon driving. Also, we find that when $\lambda = 1 \times 10^{-6}\kappa$, the PB is significantly enhanced compared to the $\lambda = 0$ case. This phenomenon results from two-photon driving, i.e., the creation of the $|00\rangle \xrightarrow{\lambda} |20\rangle$ transition. However, with the further increase of λ, two-photon driving decreases the antibunching effect. For the strong coupling, $\eta = 10\kappa$ [Figs. 9(b) and 10(b)], these results show behaviors similar to the weak-coupling case $\eta = 0.88\kappa$ [Figs. 9(a) and 10(a)]. Thus, the appropriate values of nonreciprocal coupling and two-photon driving are helpful to the enhancement of PB.

5 Experimental feasibility and conclusion

To realize a very strong PB effect under the combination of CPB and UPB, the parameter condition $\gamma < \kappa < g_j \ll \omega_{m_j}$ must be satisfied. Currently, optome-
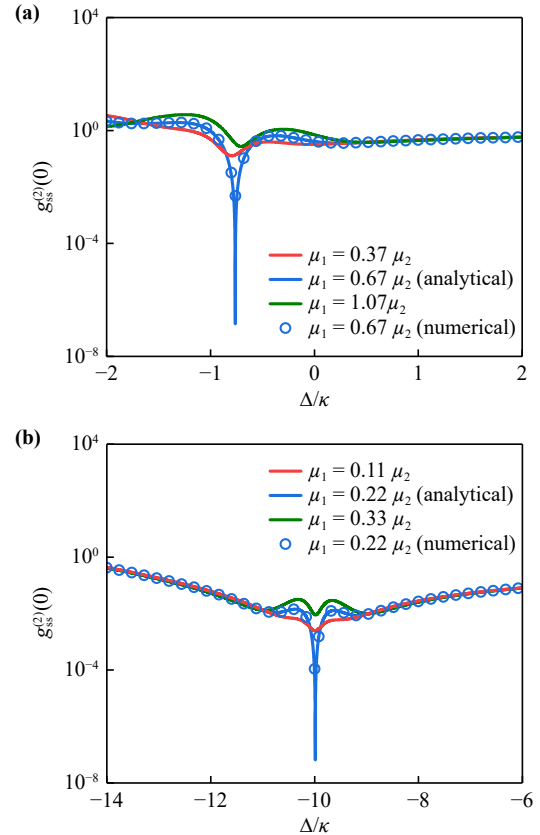
chanical systems, such as microtoroid [65], photonic and phononic crystals [66–72], membrane [73], and nanoparticle [74], have the high-frequency mechanical mode ($\sim$ GHz) and low-loss optics (or mechanics), so that the sideband resolution condition $\gamma < \kappa \ll \omega_{m_j}$ is met. Moreover, our work also needs to satisfy the single-photon strong-coupling condition $\kappa < g_j$. Experimentally, this strong coupling has been achieved in cold atoms [75–77]. Some theoretical works, including optical or mechanical parametric amplification [61, 78–80], have reported the exponentially-enhanced coupling. Therefore, our used parameters could be implemented in the currently available optomechanical systems.

In conclusion, we have investigated the CPB and the UPB in a double-cavity optomechanical system. After applying the unitary transformation and neglecting the mechanical part, we derive the effective Hamiltonian of the pure optical system. And then we verify its validity by the master equation. Specifically, we analyze the occurrence of UPB under the weak-coupling condition and the underlying physical mechanism. As the coupling strength is increasing, we find that CPB also emerges in the system. Interestingly, we discover that when the coupling between two optical cavities is reciprocal (or
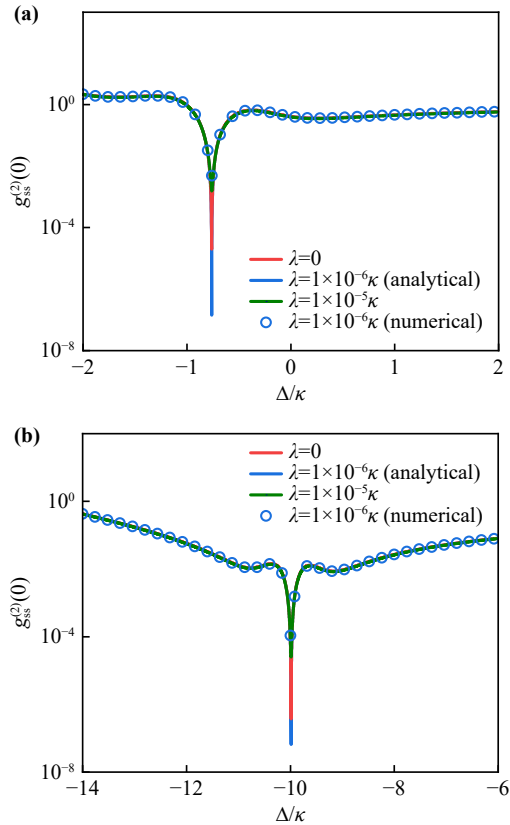
Fig. 10 The second-order correlation function $g_{ss}^{(2)}(0)$ versus the detuning Δ/κ with different values of λ. The system parameters are set as $E = 0.02\kappa$. **(a)** $\eta = 0.88\kappa$, $\mu_2 = \kappa$ and $\mu_1 \approx 0.67\mu_2$, **(b)** $\eta = 10\kappa$, $\mu_2 = 1.5\kappa$ and $\mu_1 \approx 0.22\mu_2$.

nonreciprocal), CPB and UPB can occur simultaneously in the stronger (or strong) coupling regime. The results imply that we successfully combine CPB and UPB together and utilize their respective advantages to allow one to prepare a single-photon source with high purity and high brightness. Finally, we illustrate the influences of nonreciprocal coupling and two-photon driving on the PB effect.

References

1. A. Imamoğlu, H. Schmidt, G. Woods, and M. Deutsch, Strongly interacting photons in a nonlinear cavity, *Phys. Rev. Lett.* 79(8), 1467 (1997)

2. K. M. Birnbaum, A. Boca, R. Miller, A. D. Boozer, T. E. Northup, and H. J. Kimble, Photon blockade in an optical cavity with one trapped atom, *Nature* 436(7047), 87 (2005)

3. A. Reinhard, T. Volz, M. Winger, A. Badolato, K. J. Hennessy, E. L. Hu, and A. Imamoğlu, Strongly correlated photons on a chip, *Nat. Photonics* 6(2), 93 (2012)

4. K. Müller, A. Rundquist, K. A. Fischer, T. Sarmiento, K. G. Lagoudakis, Y. A. Kelaita, C. S. Muñoz, E. del Valle, F. P. Laussy, and J. Vučković, Coherent generation of nonclassical light on chip via detuned photon blockade, *Phys. Rev. Lett.* 114(23), 233601 (2015)

5. C. Hamsen, K. N. Tolazzi, T. Wilk, and G. Rempe, Two-photon blockade in an atom-driven cavity QED system, *Phys. Rev. Lett.* 118(13), 133604 (2017)

6. A. Faraon, I. Fushman, D. Englund, N. Stoltz, P. Petroff, and J. Vučković, Coherent generation of non-classical light on a chip via photon-induced tunnelling and blockade, *Nat. Phys.* 4(11), 859 (2008)

7. C. Lang, D. Bozyigit, C. Eichler, L. Steffen, J. M. Fink, A. A. Abdumalikov, M. Baur, S. Filipp, M. P. da Silva, A. Blais, and A. Wallraff, Observation of resonant photon blockade at microwave frequencies using correlation function measurements, *Phys. Rev. Lett.* 106(24), 243601 (2011)

8. A. J. Hoffman, S. J. Srinivasan, S. Schmidt, L. Spietz, J. Aumentado, H. E. Türeci, and A. A. Houck, Dispersive photon blockade in a superconducting circuit, *Phys. Rev. Lett.* 107(5), 053602 (2011)

9. P. Rabl, Photon blockade effect in optomechanical systems, *Phys. Rev. Lett.* 107(6), 063601 (2011)

10. A. Nunnenkamp, K. Børkje, and S. M. Girvin, Single-photon optomechanics, *Phys. Rev. Lett.* 107(6), 063602 (2011)

11. A. Majumdar and D. Gerace, Single-photon blockade in doubly resonant nanocavities with second-order nonlinearity, *Phys. Rev. B* 87(23), 235319 (2013)

12. A. Miranowicz, J. Bajer, M. Paprzycka, Y. X. Liu, A. M. Zagoskin, and F. Nori, State-dependent photon blockade via quantum-reservoir engineering, *Phys. Rev. A* 90(3), 033831 (2014)

13. H. Z. Shen, Y. H. Zhou, and X. X. Yi, Quantum optical diode with semiconductor microcavities, *Phys. Rev. A* 90(2), 023849 (2014)

14. Y. P. Gao, X. F. Liu, T. J. Wang, C. Cao, and C. Wang, Photon excitation and photon-blockade effects in opto-magnonic microcavities, *Phys. Rev. A* 100(4), 043831 (2019)

15. C. Zhao, X. Li, S. Chao, R. Peng, C. Li, and L. Zhou, Simultaneous blockade of a photon, phonon, and magnon induced by a two-level atom, *Phys. Rev. A* 101(6), 063838 (2020)

16. H. Xie, L. W. He, X. Shang, G. W. Lin, and X. M. Lin, Nonreciprocal photon blockade in cavity optomagnonics, *Phys. Rev. A* 106(5), 053707 (2022)

17. Y. H. Zhou, X. Y. Zhang, Q. C. Wu, B. L. Ye, Z. Q. Zhang, D. D. Zou, H. Z. Shen, and C. P. Yang, Conventional photon blockade with a three-wave mixing, *Phys. Rev. A* 102(3), 033713 (2020)

18. T. C. H. Liew and V. Savona, Single photons from coupled quantum modes, *Phys. Rev. Lett.* 104(18), 183601 (2010)

19. M. Bamba, A. Imamoğlu, I. Carusotto, and C. Ciuti, Origin of strong photon antibunching in weakly nonlinear

012202-8

Xiang-Xiang Lu, et al., Front. Phys. 21(1), 012202 (2026)

photonic molecules, *Phys. Rev. A* 83(2), 021802(R) (2011)

20. C. Vaneph, A. Morvan, G. Aiello, M. Féchant, M. Aprili, J. Gabelli, and J. Estève, Observation of the unconventional photon blockade in the microwave domain, *Phys. Rev. Lett.* 121(4), 043602 (2018)

21. D. Gerace and V. Savona, Unconventional photon blockade in doubly resonant microcavities with second-order nonlinearity, *Phys. Rev. A* 89(3), 031803(R) (2014)

22. Y. H. Zhou, H. Z. Shen, and X. X. Yi, Unconventional photon blockade with second-order nonlinearity, *Phys. Rev. A* 92(2), 023838 (2015)

23. B. Sarma and A. K. Sarma, Quantum-interference-assisted photon blockade in a cavity via parametric interactions, *Phys. Rev. A* 96(5), 053827 (2017)

24. H. Z. Shen, C. Shang, Y. H. Zhou, and X. X. Yi, Unconventional single-photon blockade in non-Markovian systems, *Phys. Rev. A* 98(2), 023856 (2018)

25. H. Jabri and H. Eleuch, Enhanced unconventional photon-blockade effect in one- and two-qubit cavities interacting with nonclassical light, *Phys. Rev. A* 106(2), 023704 (2022)

26. Y. Qu, S. Shen, J. Li, and Y. Wu, Improving photon antibunching with two dipole-coupled atoms in whispering-gallery-mode microresonators, *Phys. Rev. A* 101(2), 023810 (2020)

27. H. J. Snijders, J. A. Frey, J. Norman, H. Flayac, V. Savona, A. C. Gossard, J. E. Bowers, M. P. van Exter, D. Bouwmeester, and W. Löffler, Observation of the unconventional photon blockade, *Phys. Rev. Lett.* 121(4), 043601 (2018)

28. X. W. Xu and Y. J. Li, Antibunching photons in a cavity coupled to an optomechanical system, *J. Phys. At. Mol. Opt. Phys.* 46(3), 035502 (2013)

29. B. Sarma and A. K. Sarma, Unconventional photon blockade in three-mode optomechanics, *Phys. Rev. A* 98(1), 013826 (2018)

30. B. Li, R. Huang, X. W. Xu, A. Miranowicz, and H. Jing, Nonreciprocal unconventional photon blockade in a spinning optomechanical system, *Photon. Res.* 7(6), 630 (2019)

31. L. J. Feng, L. Yan, and S. Q. Gong, Unconventional photon blockade induced by the self-Kerr and cross-Kerr non-linearities, *Front. Phys. (Beijing)* 18(1), 12304 (2023)

32. X. H. Fan, Y. N. Zhang, J. P. Yu, M. Y. Liu, W. D. He, H. C. Li, and W. Xiong, Nonreciprocal unconventional photon blockade with Kerr magnons, *Adv. Quantum Technol.* 7(8), 2400043 (2024)

33. X. Deng, K. K. Zhang, T. Zhang, T. Shui, and W. X. Yang, Nonreciprocal unconventional photon blockade via Barnett effect in a hybrid cavity magnonic system, *Chaos Solitons Fractals* 191, 115880 (2025)

34. J. Tang, W. Geng, and X. Xu, Quantum interference induced photon blockade in a coupled single quantum dot-cavity system, *Sci. Rep.* 5(1), 9252 (2015)

35. D. Y. Wang, C. H. Bai, S. Liu, S. Zhang, and H. F. Wang, Distinguishing photon blockade in a *PT*-symmetric optomechanical system, *Phys. Rev. A* 99(4), 043818 (2019)

36. D. Y. Wang, C. H. Bai, S. Liu, S. Zhang, and H. F. Wang, Photon blockade in a double-cavity optomechanical system with nonreciprocal coupling, *New J. Phys.* 22(9), 093006 (2020)

37. X. Liang, Z. Duan, Q. Guo, C. Liu, S. Guan, and Y. Ren, Antibunching effect of photons in a two-level emitter-cavity system, *Phys. Rev. A* 100(6), 063834 (2019)

38. C. M. Zheng, W. Zhang, D. Y. Wang, X. Han, and H. F. Wang, Simultaneously enhanced photon blockades in two microwave cavities via driving a giant atom, *New J. Phys.* 25(4), 043030 (2023)

39. F. Zou, D. G. Lai, and J. Q. Liao, Enhancement of photon blockade effect via quantum interference, *Opt. Express* 28(11), 16175 (2020)

40. E. Zubizarreta Casalengua, J. C. López Carreño, F. P. Laussy, and E. Valle, Conventional and unconventional photon statistics, *Laser Photonics Rev.* 14(6), 1900279 (2020)

41. C. J. Zhu, K. Hou, Y. P. Yang, and L. Deng, Hybrid level anharmonicity and interference-induced photon blockade in a two-qubit cavity QED system with dipole-dipole interaction, *Photon. Res.* 9(7), 1264 (2021)

42. X. Liang, Z. Duan, Q. Guo, S. Guan, M. Xie, and C. Liu, Photon blockade in a bimode nonlinear nanocavity embedded with a quantum dot, *Phys. Rev. A* 102(5), 053713 (2020)

43. Y. W. Lu, J. F. Liu, R. Li, Y. Wu, H. Tan, and Y. Li, Single-photon blockade in quasichiral atom–photon interaction: Simultaneous high purity and high efficiency, *New J. Phys.* 24(5), 053029 (2022)

44. Y. Ren, Z. Duan, B. Fan, S. Guan, M. Xie, and C. Liu, Antibunched single-photon/photon-pair emission with coupled Jaynes–Cummings model, *Opt. Express* 30(12), 21787 (2022)

45. X. Qiao, Z. Yao, and H. Yang, Strongly enhanced photon-pair blockade with three-wave mixing by quantum interference, *Phys. Rev. A* 110(5), 053702 (2024)

46. H. Zhu, X. Li, Z. Li, F. Wang, and X. Zhong, Strong antibunching effect under the combination of conventional and unconventional photon blockade, *Opt. Express* 31(13), 22030 (2023)

47. Y. H. Zhou, F. Minganti, W. Qin, Q. C. Wu, J. L. Zhao, Y. L. Fang, F. Nori, and C. P. Yang, *n*-photon blockade with an *n*-photon parametric drive, *Phys. Rev. A* 104(5), 053718 (2021)

48. Y. M. Liu, J. Cheng, H. F. Wang, and X. X. Yi, Non-reciprocal photon blockade in a spinning optomechanical system with nonreciprocal coupling, *Opt. Express* 31(8), 12847 (2023)

49. J. Y. Sun and H. Z. Shen, Photon blockade in non-Hermitian optomechanical systems with nonreciprocal couplings, *Phys. Rev. A* 107(4), 043715 (2023)

50. L. Yang, M. Mao, C. Kong, and J. Liu, Nonreciprocal coupling modulated difference-sideband generation in a double-cavity optomechanical system, *Opt. Express* 31(21), 34560 (2023)

51. N. Hatano and D. R. Nelson, Localization transitions in non-Hermitian quantum mechanics, *Phys. Rev. Lett.* 77(3), 570 (1996)

52. S. Longhi, D. Gatti, and G. Della Valle, Non-Hermitian transparency and one-way transport in low-dimensional

Xiang-Xiang Lu, et al., Front. Phys. 21(1), 012202 (2026)

012202-9

lattices by an imaginary gauge field, *Phys. Rev. B* 92(9), 094204 (2015)

53. S. Longhi, D. Gatti, and G. D. Valle, Robust light transport in non-Hermitian photonic lattices, *Sci. Rep.* 5(1), 13376 (2015)

54. J. Zhu, Ş. K. Özdemir, L. He, and L. Yang, Controlled manipulation of mode splitting in an optical microcavity by two Rayleigh scatterers, *Opt. Express* 18(23), 23535 (2010)

55. Y. Shen, M. Bradford, and J. T. Shen, Single-photon diode by exploiting the photon polarization in a waveguide, *Phys. Rev. Lett.* 107(17), 173902 (2011)

56. M. Hafezi, E. A. Demler, M. D. Lukin, and J. M. Taylor, Robust optical delay lines with topological protection, *Nat. Phys.* 7(11), 907 (2011)

57. A. Metelmann and A. A. Clerk, Nonreciprocal photon transmission and amplification via reservoir engineering, *Phys. Rev. X* 5(2), 021025 (2015)

58. S. Mancini, V. I. Man'ko, and P. Tombesi, Ponderomotive control of quantum macroscopic coherence, *Phys. Rev. A* 55(4), 3042 (1997)

59. S. Bose, K. Jacobs, and P. L. Knight, Preparation of non-classical states in cavities with a moving mirror, *Phys. Rev. A* 56(5), 4175 (1997)

60. X. W. Xu, Y. J. Li, and Y. Liu, Photon-induced tunneling in optomechanical systems, *Phys. Rev. A* 87(2), 025803 (2013)

61. X. Y. Lü, Y. Wu, J. R. Johansson, H. Jing, J. Zhang, and F. Nori, Squeezed optomechanics with phase-matched amplification and dissipation, *Phys. Rev. Lett.* 114(9), 093602 (2015)

62. R. Dum, A. S. Parkins, P. Zoller, and C. W. Gardiner, Monte Carlo simulation of master equations in quantum optics for vacuum, thermal, and squeezed reservoirs, *Phys. Rev. A* 46(7), 4382 (1992)

63. K. Mølmer, Y. Castin, and J. Dalibard, Monte Carlo wave-function method in quantum optics, *J. Opt. Soc. Am. B* 10(3), 524 (1993)

64. M. B. Plenio and P. L. Knight, The quantum-jump approach to dissipative dynamics in quantum optics, *Rev. Mod. Phys.* 70(1), 101 (1998)

65. A. Schliesser, R. Rivière, G. Anetsberger, O. Arcizet, and T. J. Kippenberg, Resolved-sideband cooling of a micromechanical oscillator, *Nat. Phys.* 4(5), 415 (2008)

66. M. Eichenfield, J. Chan, R. M. Camacho, K. J. Vahala, and O. Painter, Optomechanical crystals, *Nature* 462(7269), 78 (2009)

67. J. Chan, T. P. M. Alegre, A. H. Safavi-Naeini, J. T. Hill, A. Krause, S. Gröblacher, M. Aspelmeyer, and O. Painter, Laser cooling of a nanomechanical oscillator

68. M. J. Burek, J. D. Cohen, S. M. Meenehan, N. El-Sawah, C. Chia, T. Ruelle, S. Meesala, J. Rochman, H. A. Atikian, M. Markham, D. J. Twitchen, M. D. Lukin, O. Painter, and M. Lončar, Diamond optomechanical crystals, *Optica* 3(12), 1404 (2016)

69. A. H. Safavi-Naeini, J. Chan, J. T. Hill, T. P. M. Alegre, A. Krause, and O. Painter, Observation of quantum motion of a nanomechanical resonator, *Phys. Rev. Lett.* 108(3), 033602 (2012)

70. K. Schneider, Y. Baumgartner, S. Hönl, P. Welter, H. Hahn, D. J. Wilson, L. Czornomaz, and P. Seidler, Optomechanics with one-dimensional gallium phosphide photonic crystal cavities, *Optica* 6(5), 577 (2019)

71. L. Qiu, I. Shomroni, P. Seidler, and T. J. Kippenberg, Laser cooling of a nanomechanical oscillator to its zero-point energy, *Phys. Rev. Lett.* 124(17), 173601 (2020)

72. J. Kolvik, P. Burger, J. Frey, and R. Van Laer, Clamped and sideband-resolved silicon optomechanical crystals, *Optica* 10(7), 913 (2023)

73. J. C. Sankey, C. Yang, B. M. Zwickl, A. M. Jayich, and J. G. E. Harris, Strong and tunable nonlinear optomechanical coupling in a low-loss system, *Nat. Phys.* 6(9), 707 (2010)

74. N. Meyer, A. R. Sommer, P. Mestres, J. Gieseler, V. Jain, L. Novotny, and R. Quidant, Resolved-sideband cooling of a levitated nanoparticle in the presence of laser phase noise, *Phys. Rev. Lett.* 123(15), 153601 (2019)

75. F. Brennecke, S. Ritter, T. Donner, and T. Esslinger, Cavity optomechanics with a Bose-Einstein condensate, *Science* 322(5899), 235 (2008)

76. K. W. Murch, K. L. Moore, S. Gupta, and D. M. Stamper-Kurn, Observation of quantum-measurement back-action with an ultracold atomic gas, *Nat. Phys.* 4(7), 561 (2008)

77. T. P. Purdy, D. W. C. Brooks, T. Botter, N. Brahms, Z. Y. Ma, and D. M. Stamper-Kurn, Tunable cavity optomechanics with ultracold atoms, *Phys. Rev. Lett.* 105(13), 133602 (2010)

78. M. A. Lemonde, N. Didier, and A. A. Clerk, Enhanced nonlinear interactions in quantum optomechanics via mechanical amplification, *Nat. Commun.* 7(1), 11338 (2016)

79. T. S. Yin, X. Y. Lü, L. L. Zheng, M. Wang, S. Li, and Y. Wu, Nonlinear effects in modulated quantum optomechanics, *Phys. Rev. A* 95(5), 053861 (2017)

80. L. J. Feng and S. Q. Gong, Two-photon blockade generated and enhanced by mechanical squeezing, *Phys. Rev. A* 103(4), 043509 (2021)

into its quantum ground state, *Nature* 478(7367), 89 (2011)

012202-10

Xiang-Xiang Lu, et al., Front. Phys. 21(1), 012202 (2026)